Thermal and Photochemical Stability Studies of Color-Converted MicroLED Microdisplay Panels

Asim M. Noor Elahi, Zengzhi Pei, Peichen Yu, and Jian Xu

***Abstract*—The thermal and photochemical stabilities of colloidal quantum-dot (QD) nanophosphors incorporated into a blue microLED matrix by spin-cast deposition were investigated in this study. The optical characteristics of QDs-based color-converted microLEDs were also investigated in this study. The measurements performed in this work suggest the ultimate limit of QD performance in microLED devices. The findings from the stability evaluations encourage and motivate the employment of red, green QD color converters in blue microLED matrices to create full-color microLED devices. Such studies will be helpful in the design and the fabrication of high-efficiency and high-performance micro-LED microdisplay panels**

***Index Terms*—Color-converted MicroLEDs, quantum dots, QD nanophosphors, thermal stability, photochemical stability, colorful MicroLED microdisplay panels.**

I. Introduction

DEVELOPING full-color microLED arrays by incorporating colloidal Quantum Dot (QD) into microLED matrices as color converters has shown great promises in the development of next-generation microdisplay panels in the coming era of wearable electronics, where augmented-reality smart glasses and virtual-reality headsets will be massively adopted [1], [2]. In QDs, the strong quantum confinement of those zero-dimension nanostructures makes it possible to tune the QD emission over the entire visible color band simply by varying the particle size, which imparts tremendous spectral control for the down-conversion QD phosphors [3], [4]. Moreover, the sub-10 nanometer size of many colloidal QDs completely eliminates the light scattering problem of the conventional Y3Al5O12:Ce3+ crystals [5]. Additionally, the narrow-emission spectra, the wide color gamut, and the high quantum yield of the QDs make those emissive materials the most promising phosphor candidate for microLED based display devices [6]. Recently, color-converted microLED display panels have been fabricated using QD nanophosphors [7], showing high contrast, low cross talk and a gamut of ∼92% of DCI-P3 standard. Fig. 1 depicts images that were processed through a white microLED display panel developed in this study, featuring QD nanophosphor-based color conversion, 12 micrometer pixels and a resolution of 960 × 540. All of the different colors can then be generated from the white microLED display panel by utilizing RGB patterned filters.

Despite all of the aforementioned merits, the instability of QD nanophosphors is still a serious concern for the implementation of those emissive materials in the microLED display panels, leading to phosphor quenching which results from deteriorated QD materials. It is well known that QDs are degraded by atmospheric conditions (water, Oxygen, and ultra-violet (UV) exposure). Exposing the QDs for long time to oxygen molecules induce the reversable formation of traps on the surface of the QDs [6], [8]. It also causes a reduction in the core size, spectrum broadening, and a shift of the band-edge emission since the surface traps increase the non-radiative Auger recombination and hence reduce the stability of the QDs [6], [8], [9], [10]. Furthermore, thermal heating can also quench the QDs' photoluminescence (PL) emission. It is caused by thermally produced transitory trap states that are reversible up to a specific temperature [6], [9]. Once the temperature has returned to room temperature, the PL emission of the QDs can be restored to its prior state before heating the QDs. However, those temporary trap states can become permanent trap states by cyclic overheating and cooling of the QDs [6], [9].

Operation of microLED display panels under high brightness conditions is inevitably accompanied with temperature elevation, and there have been very few reports that studied the effect of the thermal and photochemical stability of QDs that are embedded in the microLED device structures [5], [6]. Therefore, it is the purpose of this work to investigate and study the thermal and photochemical stabilities of the red and green QD nanophosphor layers embedded in microLED matrices along with their optical characteristics to determine the operating efficiency limit of such devices. Such studies will be helpful for designing and fabricating high-efficiency and high-performance micro-LED display panels. The Experimental procedures for fabricating the full color microLED arrays are provided in Section II. Results are presented and discussed in Section III, and the Conclusion is presented in Section IV.

II. Experimental Procedures

The (In,Ga)N microLED chip contains an array of micro-LEDs with 25 μm × 25 μm square mesa shapes and

Manuscript received 26 March 2023; revised 21 May 2023; accepted 26 May 2023. Date of publication 31 May 2023; date of current version 8 June 2023. *(Corresponding author: Jian Xu.)*

Asim M. Noor Elahi is with the Photonic and Optoelectronic Devices group, Department of Engineering Science and Mechanics, Pennsylvania State University, University Park, PA 16802 USA., and also with the Electrical Engineering Department, Faculty of Engineering, Taibah University, Madinah 42353, Saudi Arabia (e-mail: amn201@psu.edu).

Zengzhi Pei and Jian Xu are with the Photonic and Optoelectronic Devices group, Department of Engineering Science and Mechanics, Pennsylvania State University, University Park, PA 16802 USA (e-mail: zzp49@psu.edu; jxx10@psu.edu).

Peichen Yu is with the Green Photonics Laboratory, Department of Photonics, National Chiao-Tung University, Hsinchu 30010, Taiwan (e-mail: peichen.yu@nycu.edu.tw).

Digital Object Identifier 10.1109/JPHOT.2023.3281571

(a)

(b)

Fig. 1. Some images that were processed through a white microLED display panel with 12 micrometer pixels and a resolution of 960 × 540.

30 μm pitch. Those microLEDs were patterned into the matrix dimensions of 500 × 300 and were fabricated on 2-inch commercial LED epi-wafers that were grown on c-face (0001) sapphire substrates by metal organic chemical vapor deposition (MOCVD). The epitaxial structure of those devices comprises, from bottom to top, a $\sim$ 2.5 μm unintentionally-doped ($N_d \approx 3 \times 10^{16}$ cm^{-3}) GaN layer on top of a sapphire substrate, a $\sim$ 2.4 μm n-type ($N_d \approx 1 \times 10^{18}$ cm^{-3}) GaN layer, a $\sim$ 125 nm multiple quantum well (MQW) emissive layer consisted of fifteen pairs of $In_{0.1}Ga_{0.9}N$/GaN, a $\sim$ 200 nm p-type GaN layer ($N_A \approx 5 \times 10^{17}$ cm^{-3}), and a $\sim$ 200 nm p$^+$-type GaN capping layer ($N_A > 1 \times 10^{18}$ cm^{-3}). The fabrication process starts with a dry etching using a Cl2/Ar inductively coupled plasma (ICP) cyclic etching process to expose the nGaN layer for the formation of the Ohmic contacts. Then, ICP etching is performed to the u-GaN for device isolation. When compared to conventional reactive ion etching (RIE) techniques, ICP reactive ion etching (RIE) provides more anisotropic etch profiles and low-damage high etch rates. The etching depth for device isolation is $\sim$ 1.2 μm, which also exposes the n-type GaN contact region. After the etching process, the samples are exposed to (0.1-1) mole/L aqueous KOH solution for extended time to eliminate significant amount of the surface defects produced by the ICP etching process and also to reduce the leakage current.

Following the KOH treatment, the samples are annealed for 2 minutes in nitrogen using a rapid thermal annealing (RTA) tool at a flow rate of 5 sccm and a temperature of 700 °C. Ohmic contact consists of Ti/Al/Ti/Au with thicknesses of (10 nm/40 nm/40 nm/200 nm) and indium tin oxide (ITO) with a thickness of (300 nm) were e-beam evaporated over the n-GaN and p-GaN surfaces of the microLEDs, respectively, and then annealed using RTA in nitrogen at temperature 500 °C for 1 min to form n-type and p-type Ohmic electrodes [11], [12], [13].

To fabricate the colorful microLEDs, the sapphire substrate of the flip-chip bonded microLED sample was first removed using laser lift-off (LLO). The fabricated microLED array sample was subsequently flip-chip bonded to a silicon substrate with patterned Au/Cr electrodes for addressing a set of pre-defined subarrays of microLEDs during lighting test. Following LLO processing, a Red-Green QD film was solution-cast deposited over the GaN layer of the micro-LED structure that had been exposed to air. To prepare the QD-PMMA films, the QD chloroform solution was combined with a chloroform solution containing polymethyl methacrylate (PMMA) at predetermined concentrations and solution ratios. The weight ratio of 1:7 for red and green QDs in the QD-PMMA chloroform solution was used to balance correlated color temperature (CCT) and color rendering index (CRT). Finally, QD-PMMA thin films were produced from spin-cast deposition from the solution. A nominal QD film thickness of $\sim$15 micrometer was achieved by combined-tuning of PMMA concentration in the solution and spin speed. The QDs film contains red and green emitting CdSe/CdS nanocrystals in (PMMA) host matrix, forming a composite phosphor layer of high optical transparency with negligible scattering. This composite phosphor layer of high optical transparency with negligible scattering is necessary to retain the high emission resolution of the underlying blue microLED array panel at ambient temperature. The weight ratio of 1:7 for red and green QDs in the QD-PMMA film was chosen for balanced color temperature and color rendering index based on the previous experimental colometric studies of the fluorescence emission of the mixed red and green QDs in PMMA. Fig. 2 presents the schematic structure of the microLED array and the inset picture is the colorful microLED sample used for the performed experiments in this study. All The optical characteristics of the devices (including spectral power

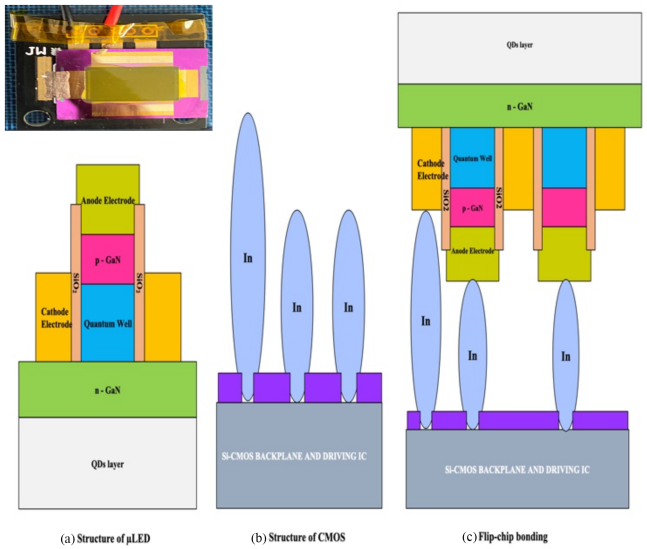

Fig. 2. Schematic structure of the micoLED devices. The inset picture is the colorful microLED sample used for the performed experiments that will be mentioned in the manuscript.

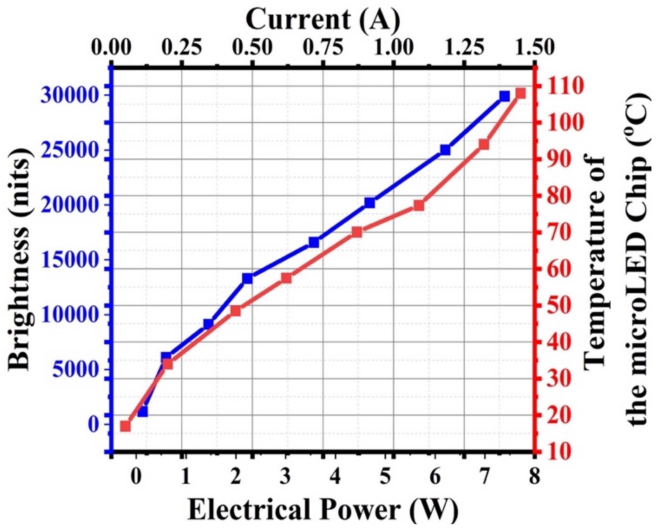

Fig. 3. Real Brightness (in nits) and the temperature associated with the applied electrical power on the microLED chip that is mounted on the Thermoelectric cooler with a fixed temperature of 15 °C.

distribution, chromaticity coordinates, correlated color temperature, color rending index (Ra)) in this work were measured at room temperature with Relative humidity between 30% to 50% using HP8000 LED fast-scan micro-spectrophotocolorimeter system, TES-137 Luminance Meter, and the temperature of the devices was measured using a k-type thermocouple attached to a Proster Digital Temperature Thermometer.

III. Results and Discussions

One of the most important characteristics of the microLED arrays is that it can achieve higher brightness in cd/m^2 (nits) compared to OLED technologies particularly in the application of micro-displays. For example, in the applications of smart glasses (AR/VR applications), or in any optical micro-display systems with OLED technologies, the up-to-date peak brightness of a colorful micro-display made with OLED technology didn't exceed 5000 cd/m^2 (nits) [14], [15]. Also, Since the efficiency of the near-eye projection and combiner systems used in those applications remains low (∼5-10%) [16], [17], it is almost impossible to present the digital image (information) superimposed on the ambient brightness which is typically around 1000 – 1500 nits with a 5000 nits background of the OLED technology if those applications are worn during the daytime. Therefore, a brightness of 5000 nits is still inadequate for the applications of AR/VR technologies with bad optical systems efficiency.

To overcome this problem, the brightness of the micro-display should be increased to at least multiple folds higher than the peak brightness of OLED micro-display which can be achieved by using white color microLED arrays instead of white OLED technology in those applications. Fig. 3 depicts the capability of realizing 30000 nits using the fabricated microLED arrays employed in this study. It can be noticed from the figure that the electrical current used to drive the microLED sample is high in order to reach to at least to 30000 nits, indicating that the device has undergone a thermal stress to achieve that desired brightness. In our stress study, the fabricated chip was back mounted on a thermoelectric cooler using an adhesive thermal paste with a fixed temperature of 15 °C to protect the LED pixels from being burned up by the high electrical power applied to the microLED array sample. Using the thermoelectric cooler at 15 °C kept the surface temperature of the device below 115 °C while achieving a brightness of 30000 nits as it can be seen from Fig. 3. It is worth noting that the microLED arrays used in the present study were driven in direct current (DC) mode and are not optimized. So, there are still plenty of rooms for improving efficiency of those microLED devices.

As a higher electrical current is injected into the sample, the LED junction temperature increased, which elevates the working temperature of the QD color conversion layer and hence, the efficiency of the QDs drops due to the formation of temporary trap states that are created by the thermal heating. Those trap states are created by the displacement of surface atoms (column VI materials such as S or Se atoms in CdSe, CdS, or ZnS QDs) from their regular arrangement at high temperature. The displacement of surface atoms at substantially high temperatures creates more vacancies by leaving behind uncompensated (zinc or cadmium) atoms on the surface that act as trap sites for electron charges and hence, the drop of the QDs efficiency occurs due to the trap emission or nonradiative recombination of these trap states [6], [9]. Fig. 4(a) shows the relative drop of the QDs efficiency at the increase of the temperatures of the white microLED chip that is mounted on a thermoelectric cooler with a fixed sink temperature of 15 °C. The QDs efficiency is normalized to 100% at room temperature for the sake of comparison. When the measured temperature rises to roughly 70 °C, the efficiency of the QDs reduces to around 58%, and it remains stable around that state even when the temperature rises to around 80 °C. However, after switching off the applied electrical power on the device, the

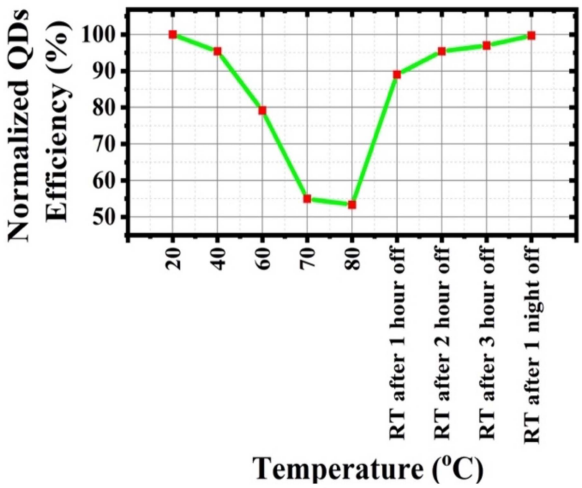

(a)

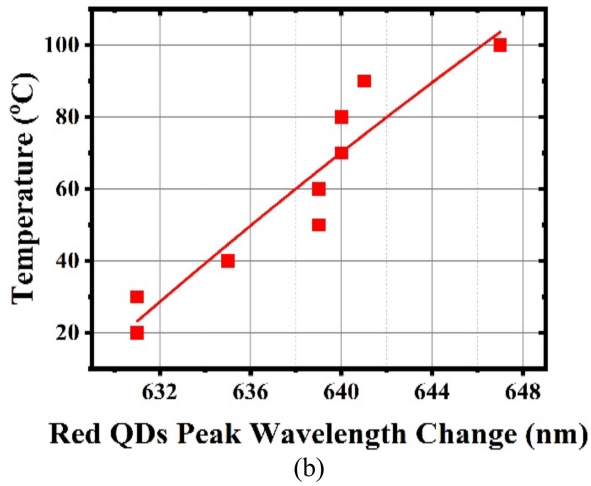

(b)

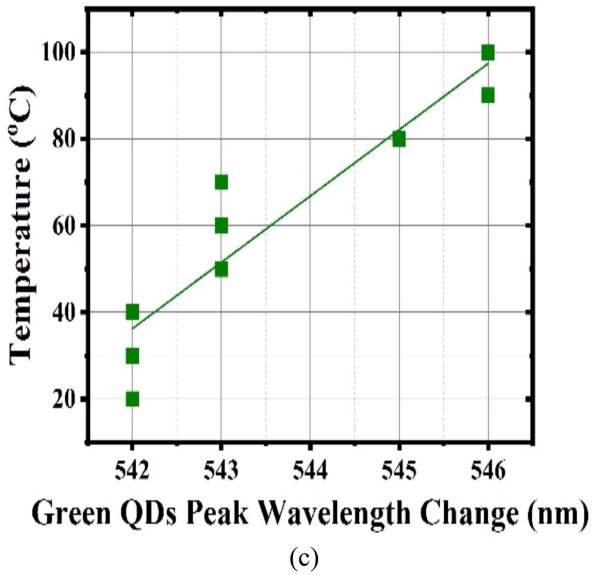

(c)

Fig. 4. (a) (top) QDs efficiency at different temperatures of the microLED chip that is mounted on the Thermoelectric cooler with a fixed temperature of 15 °C. (b) (middle) Red & (c) (bottom) green QDs peak wavelengths shifts with the temperature increase.

efficiency of the QDs progressively returns to its former state, and fully recovers after 1 night of having the device cooled down to room temperature. It is speculated that the vacancies created by the displacement of the cadmium atoms are filled back in as the surface atoms revert to their original arrangement with switching off the applied electrical power on the microLED chip. Fig. 4(b) and (c) depict the maximum wavelengths shift of the green and red QDs with the change of the temperature of the device. It can be noticed from the figures that the red QDs peak wavelength change significantly as the temperature increases compared to the green QDs peak wavelength which can affect the overall color of the microLED arrays that are utilized in the application of displays technologies.

The correlated color temperature of the sample is another key component that is altered by increasing the electrical power. Fig. 5(a) illustrates the measured (using the integration sphere) and estimated (using the McCamy approximation) correlated color temperature of the white microLED arrays in Kelvin as a function of the electrical power delivered to the device. The inset pictures are the white color from the microLED device for an electrical power of 0.13 W. The standard color temperature for bright white in display applications is in between 4000 and 6000 K [18]. It can be noticed from the figure that the color temperature of the device at 0.13 W is around 4400 K, and as the electrical power increases, the color temperature advances towards the blue color temperature region. This is mainly due to the fact that as the current increases, the device's temperature rises, the QDs degrade, and the device's efficiency decreases; as a result, the device's color temperature is dominated by the blue color from the microLED chip. The figure also shows a great agreement between the measured values of the color temperature from integration sphere and the calculated color temperature values from McCamy formulas that is given by [19]:

$$CCT = an^3 + bn^2 + cn + d \tag{1}$$

Where $a,\ b,\ c,\ and\ d$ are constants values that resulted from solving his third polynomial equation to calculate the CCT from (CIE 1931, x, y), n is the inverse line slope of the iso-temperature line from a convergence point to the chromaticity of the light and it is given by [19]:

$$n = (x - x_e) / (y - y_e) \tag{2}$$

Where $x_e$and y_e are the best-fit CCT epicenter that was determined from the intersections of 16 pairs of CCT iso-temperature lines between 2222 and 12500 K that provided the least CCT errors in that range and their values are 0.3320 and 0.1858, respectively. The coordinates of the color temperature (CIEx, CIEy) employed in the inverse slope equation were found from the integration sphere ranging from (0.351, 0.3275) at 0.13 W to (0.2756, 0.362) at 7.4 W. The change of CIE coordinates is illustrated in the CIE chart as shown in Fig. 5(b).

Furthermore, the photochemical stability of the microLED phosphor has also been investigated in this work by exposing the QD films over the pixelated microLEDs to a known intensity of blue microLED lights for particular time periods and evaluating

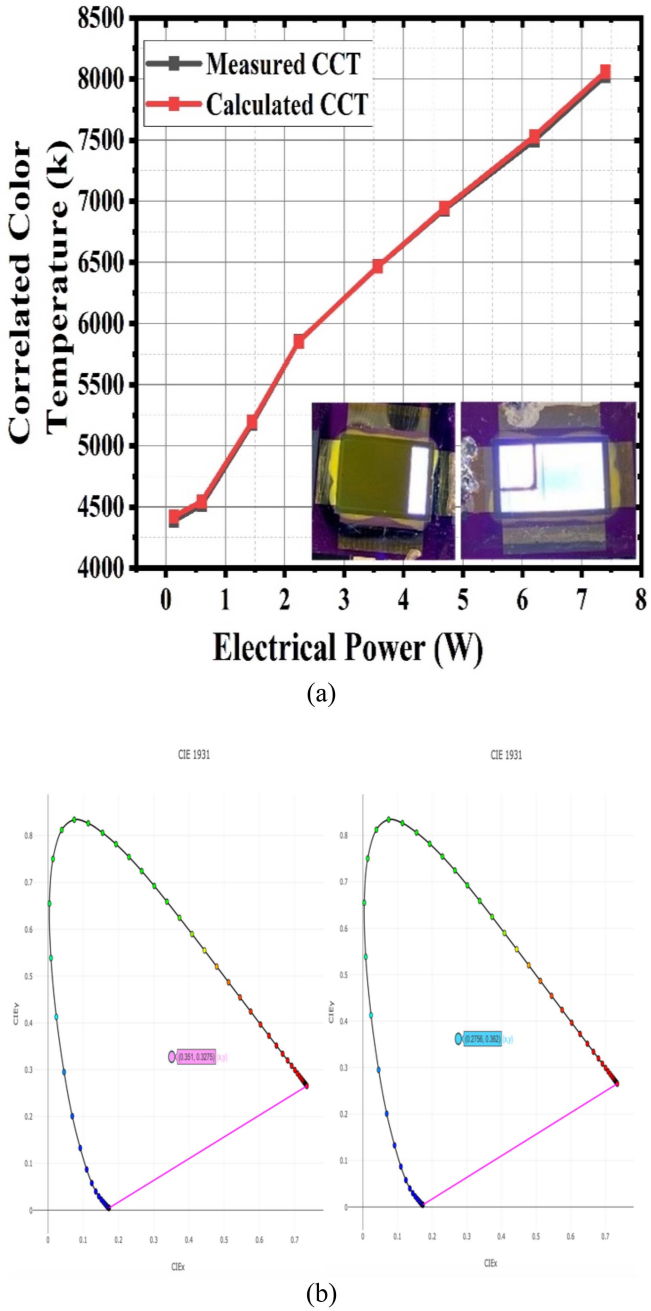

Fig. 5. (a) Correlated color temperature of the colorful microLED pixels in Kelvin associated with the electrical power applied on the device. The inset pictures are the white color from the microLED device for an electrical power of 0.13 W. (b) The change of CIE coordinates in the CIE Chart at 0.13 W (left) and at 7.4 W (right).

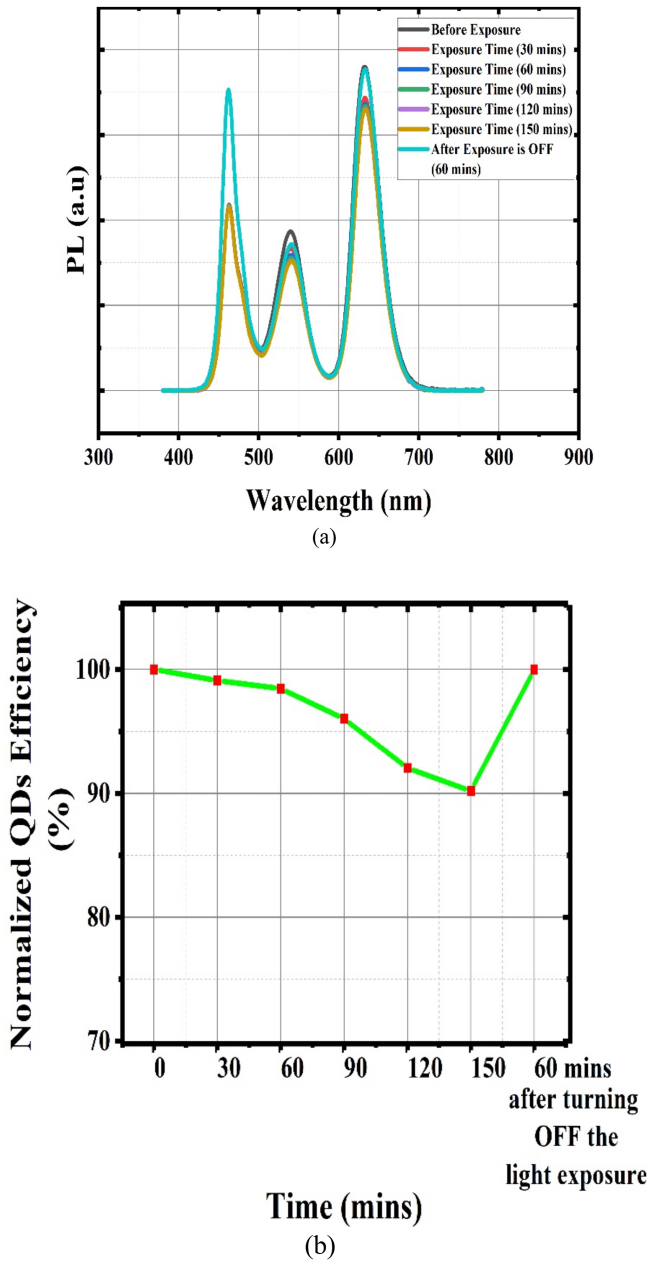

Fig. 6. (a) PL measurement of different time exposure to blue microLED light. (b) The QDs quantum yield at different working times for an applied voltage of 3 V and the current of 0.1 A and the temperature of the sample was at 22 °C.

the QDs efficiency during that time. Fig. 6(a) and (b) show the PL intensity and normalized quantum yield (QY) of the QDs film when the blue microLED light was turned on at an electrical power of 0.13 W and the device's temperature was steady at room temperature. This study shows that the sample was only turned on for almost 3 hours which could be considered as the average duration of using some of the applications in a single day (e.g., TV). The figures depict that both the PL intensity and the normalized QY of the QD layers are decreased as the exposure time increases. This reduction of the QDs efficiency has been reported to be attributed to the formation of reversible traps on the surface of the QDs as a result of oxygen molecule exposure [6], [8]. Photooxidation produces ions such as SeO_3 and Cd_2^+ that dissociate from the core in the presence of oxygen and under the blue light illumination of the microLED pixels. When the sample exposed to oxygen for extended periods of time, more traps build on the surface, causing permanent fluorescence quenching [6], [9]. However, Fig. 6(b) shows that after turning off the blue light for an hour, the QDs efficiency largely restored to its original efficiency which can be considered promising results for colorful

microLED devices as the QDs can reinstate their performance in a very short time of turning off the blue light, implying that even after 3 hours of microLED operation in the presence of oxygen, there were not many traps to permanently quench the florescence. This might be because the QDs' outer-shell thickness is high which has been claimed to play an essential role in boosting QD stability. QDs with thicker outer shells diminish surface trap states and inhibit dot-to-dot energy transfer, lowering non-radiative Auger recombination and improving the QDs stability [10].

Because the microLED sample in this study are not optimized and their efficiencies are much lower than the state-of-the-art standard microLED efficiencies, these results are promising and motivating for the purpose of using the mix of green and red QDs layers in blue microLED matrices to achieve full-color microLED devices.

IV. Conclusion

The thermal and photochemical stability of mixed red and green QD nanophosphors incorporated into microLED matrices, as well as their optical properties, have been investigated in order to estimate the operational efficiency limit of such devices. The results reveal that the PL intensity of QDs decreases after blue light exposure but recovers after relaxing. Also, the same behavior was observed after cooling down the sample after applying thermal stress to the device. The mechanisms behind these phenomena have been discussed and explained in this paper. These results have opened many prospects for the design and fabrication of colorful microLED devices for the applications of micro-display panels because the devices utilized in this study are not optimized and there are still a lot of opportunities for increasing the optimization of those microLED devices.

Acknowledgment

A. M. NE thanks the Ministry of Education in Saudi Arabia through Taibah University for funding all of his research courses and activities which include the exerted effort in this work.

References

[1] Y. Huang et al., "Mini-LED, Micro-LED and OLED displays: Present status and future perspectives," *Light, Sci. Appl.*, vol. 9, no. 1, pp. 105–105, 2020.
[2] T. Wu et al., "Mini-LED and Micro-LED: Promising candidates for the next generation display technology," *Appl. Sci.*, vol. 8, no. 9, 2018, Art. no. 1557.
[3] Z. Liu et al., "Micro-light-emitting diodes with quantum dots in display technology," *Light, Sci. Appl.*, vol. 9, no. 1, 2020, Art. no. 83.
[4] Y. Huang et al., "Advances in quantum-dot-based displays," *Nanomater*, vol. 10, no. 7, 2020, Art. no. 1327.
[5] P. F. Smet, A. B. Parmentier, and D. Poelman, "Selecting conversion phosphors for white light-emitting diodes," *J. Electrochem. Soc.*, vol. 158, no. 6, pp. R37–R54, 2011.
[6] H. Moon et al., "Stability of quantum dots, quantum dot films, and quantum dot light-emitting diodes for display applications," *Adv. Mater*, vol. 31, no. 34, 2019, Art. no. e1804294-n/a.
[7] F. Gou et al., "High performance color-converted microLED dsiplay," *J. Soc. Inf. Display*, vol. 27, pp. 199–206, 2019.
[8] S. R. Cordero et al., "Photo-activated luminescence of CDSE quantum dot monolayers," *J. Phys. Chem. B*, vol. 104, no. 51, pp. 12137–12142, 2000.
[9] J. Ko et al., "Chemically resistant and thermally stable quantum dots prepared by shell encapsulation with cross-linkable block copolymer ligands," *NPG Asia Mater.*, vol. 12, no. 1, 2020, Art. no. 19.
[10] Y. Fu et al., "Excellent stability of thicker shell CdSe@ZnS/ZnS quantum dots," *RSC Adv.*, vol. 7, no. 65, pp. 40866–40872, 2017.
[11] M. R. M. Atalla et al., "On the design of GaN vertical MESFETs on commercial LED sapphire wafers," *Solid-State Electron.*, vol. 126, pp. 23–31, 2016.
[12] A. M. Noor Elahi et al., "The effect of the undoped GaN/buffer-layer interface on the operation of Schottky diodes and MESFET devices," *Microelectronic Eng.*, vol. 214, pp. 38–43, 2019.
[13] J. Liu et al., "Alternating current III-nitride light-emitting diodes with on-chip Schottky barrier diode rectifiers," *IEEE Trans. Electron Devices*, vol. 66, no. 9, pp. 3881–3886, Sep. 2019.
[14] J. Hamer et al., "12-2: High-performance OLED microdisplays made with multi-stack OLED formulations," *Proc. SPIE*, vol. 11473, 2020, Art. no. 114730F.
[15] Y. Huang et al., "Mini-LED, Micro-LED and OLED displays: Present status and future perspectives," *Light, Sci. Appl.*, vol. 9, no. 1, pp. 105–105, 2020.
[16] T. Zhan et al., "Augmented reality and virtual reality displays: Perspectives and challenges," *Iscience*, vol. 23, no. 8, pp. 101397–101397, 2020.
[17] C. Chang et al., "Toward the next-generation VR/AR optics: A review of holographic near-eye displays from a human-centric perspective," *Optica*, vol. 7, no. 11, pp. 1563–1578, 2020.
[18] G. S. Archer, "Color temperature of light-emitting diode lighting matters for optimum growth and welfare of broiler chickens," *Animal*, vol. 12, no. 5, pp. 1015–1021, 2018.
[19] J. Hernandez-Andres et al., "Calculating correlated color temperatures across the entire gamut of daylight and skylight chromaticities," *Appl. Opt.*, vol. 38, pp. 5703–5709, 1999.